

Article

Photoproduction of Heavy Meson and Photon Pairs

Marat Siddikov

Special Issue

Selected Papers from the 13th International Conference on New Frontiers in Physics (ICNFP 2024)

Edited by

Prof. Dr. Larissa Bravina, Prof. Dr. Sonia Kabana and Prof. Dr. Armen Sedrakian



Article

Photoproduction of Heavy Meson and Photon Pairs

Marat Siddikov 

Departamento de Física, Universidad Técnica Federico Santa María, y Centro Científico-Tecnológico de Valparaíso, Casilla, Valparaíso 110-V, Chile; marat.siddikov@usm.cl

Abstract: The extraction of the Generalized Parton Distributions of the nucleons from phenomenological analyses of experimental data presents a challenging problem which is being actively studied in the literature. Due to theoretical limitations of some of the well-known channels, currently many new processes are being analyzed in the literature as potential novel probes. In this proceeding we propose to use the exclusive photoproduction of $\eta_c\gamma$ pairs as a new channel for study of the GPDs. Our analysis shows that this process is primarily sensitive to the unpolarized gluon GPDs H_g in the Efremov-Radyushkin-Brodsky-Lepage (ERBL) kinematics. The numerical estimates of the cross-section and the expected counting rates for middle-energy photoproduction experiments show that expected counting rates are sufficiently large for a dedicated experimental study at the future Electron-Ion Collider (EIC) or in ultraperipheral collisions at the LHC. The total (integrated) photoproduction cross-section $\sigma_{\text{tot}}^{\gamma p \rightarrow \gamma \eta_c p}$ in this kinematics scales with energy W as $\sigma_{\text{tot}}^{\gamma p \rightarrow \gamma \eta_c p}(W, M_{\gamma \eta_c} \geq 3.5 \text{ GeV}) \approx 0.48 \text{ pb} \left(\frac{W}{100 \text{ GeV}}\right)^{0.75}$, and yields a few thousands of events per 100 fb^{-1} of the integrated luminosity.

Keywords: generalized parton distributions; proton tomography; exclusive photoproduction

1. Introduction

The Generalized Parton Distributions (GPDs) encode a crucial information about the nonperturbative dynamics of the partons in hadrons, and for this reason have been a subject of extensive theoretical and experimental research [1–6]. Since the GPDs cannot yet be calculated from the first principles, at present they are extracted from the phenomenological analyses of experimental data, primarily the $2 \rightarrow 2$ processes like Deeply Virtual Compton Scattering (DVCS) and Deeply Virtual Meson Production (DVMP). However, these channels do not fully constrain the GPDs [7–9]. The phenomenological uncertainties are especially pronounced in the Efremov-Radyushkin-Brodsky-Lepage (ERBL) kinematics, for gluon GPDs and for transversity sector. This has prompted a search for new experimental channels, particularly $2 \rightarrow 3$ processes [10–25], which may provide complementary information by targeting different GPD flavor combinations across different kinematic regions. In this proceeding we propose to use the exclusive photoproduction of heavy quarkonia-photon pairs as a promising tool for studies of the gluon GPDs. The heavy mass of the quarkonia provides a natural hard scale, justifying the perturbative techniques even in the photoproduction regime, while avoiding soft and collinear singularities inherent in processes with massless quarks. The hadronization of the quark-antiquark pair into quarkonium is described within the NRQCD framework [26–28], allowing for systematic inclusion of the perturbative corrections. The photoproduction of heavy quarkonia has been understood reasonably well from the extensive studies of the $2 \rightarrow 2$ processes (e.g., $\gamma p \rightarrow J/\psi p$). However, these processes share the limitations of all $2 \rightarrow 2$ processes like



Academic Editors: Armen Sedrakian, Larissa Bravina and Sonia Kabana

Received: 31 December 2024

Revised: 8 February 2025

Accepted: 26 February 2025

Published: 3 March 2025

Citation: Siddikov, M.

Photoproduction of Heavy Meson and Photon Pairs. *Particles* **2025**, *8*, 23.

<https://doi.org/10.3390/particles8010023>

Copyright: © 2025 by the authors. Licensee MDPI, Basel, Switzerland. This article is an open access article distributed under the terms and conditions of the Creative Commons Attribution (CC BY) license (<https://creativecommons.org/licenses/by/4.0/>).

DVCS and DVMP. In this context, the process $\gamma p \rightarrow \eta_c \gamma p$ deserves attention as a novel probe of the gluon GPDs, which are defined below in [25,26]. In order to minimize contamination by feed-down contributions (from decays of heavier quarkonia), we will focus on the kinematics of large invariant mass of $\eta_c \gamma$. This kinematic regime can be explored in low- and middle-energy photon-proton collisions at the LHC, the future Electron Ion Collider (EIC), and potential experiments at JLAB after a 22 GeV upgrade. The $\eta_c \gamma$ pair photoproduction also deserves attention as a possible background to η_c photoproduction ($\gamma p \rightarrow \eta_c p$), which has been extensively studied as a promising channel for detecting odderons. Unlike η_c photoproduction, the $\eta_c \gamma$ pair photoproduction does not require C-odd exchanges in the t -channel, and thus might give a significant background that could limit the detectability of odderons in future experiments focusing on η_c photoproduction.

2. Amplitude of the Process in the Collinear Factorization Framework

The analysis of $\eta_c \gamma$ -photoproduction in the collinear factorization approach largely follows similar studies of the photoproduction of light meson-photon pairs ($\gamma\pi$, $\gamma\rho$) discussed in [10,11]. However, the meson mass M_{η_c} in such analysis cannot be disregarded and must be treated as a hard scale, on par with the invariant mass $M_{\gamma\eta_c}$ of the photon-meson pair. Since the flux of equivalent photons in electro- and ultraperipheral hadroproduction experiments is dominated by quasi-real photons, in what follows we'll focus on photoproduction by transversely polarized onshell photons. In what follows we will perform the evaluations in the photon-proton collision frame, although our final results for the invariant cross-sections does not depend on this choice. The light-cone components (v^+ , v^- , v_\perp) of all the particles' momenta in this frame can be parametrized as [12]

$$q^\mu = \left(\sqrt{\frac{s}{2}}, 0, \mathbf{0}_\perp \right) \quad (1)$$

$$P_{\text{in}}^\mu = \left(\frac{m_N^2}{\sqrt{2s}(1+\xi)}, (1+\xi)\sqrt{\frac{s}{2}}, \mathbf{0}_\perp \right), \quad (2)$$

$$P_{\text{out}}^\mu = \left(\frac{m_N^2 + \Delta_\perp^2}{\sqrt{2s}(1-\xi)}, (1-\xi)\sqrt{\frac{s}{2}}, \Delta_\perp \right), \quad (3)$$

$$\Delta^\mu = P_{\text{out}}^\mu - P_{\text{in}}^\mu = \left(\frac{2\xi m_N^2 + (1+\xi)\Delta_\perp^2}{\sqrt{2s}(1-\xi^2)}, -2\xi\sqrt{\frac{s}{2}}, \Delta_\perp \right) \quad (4)$$

$$p_{\eta_c}^\mu = \left(\alpha_{\eta_c} \sqrt{\frac{s}{2}}, \frac{\left(\mathbf{p}_\perp^{\eta_c} \right)^2 + M_{\eta_c}^2}{\alpha_{\eta_c} \sqrt{2s}}, \mathbf{p}_\perp^{\eta_c} \right), \quad \mathbf{p}_\perp^{\eta_c} := -\mathbf{p}_\perp - \frac{\Delta_\perp}{2} \quad (5)$$

$$k^\mu = \left((1 - \alpha_{\eta_c}) \sqrt{\frac{s}{2}}, \frac{\left(\mathbf{k}_\perp^\gamma \right)^2}{(1 - \alpha_{\eta_c}) \sqrt{2s}}, \mathbf{k}_\perp^\gamma \right), \quad \mathbf{k}_\perp^\gamma := \mathbf{p}_\perp - \frac{\Delta_\perp}{2} \quad (6)$$

$$\mathbf{p}_\perp \equiv \left(\mathbf{k}_\perp^\gamma - \mathbf{p}_\perp^{\eta_c} \right) / 2 \quad (7)$$

where q^μ and k^μ are the momenta of the incoming and outgoing (scattered) photon, $p_{\eta_c}^\mu$ is the four-momentum of the produced quarkonia, and P_{in}^μ , P_{out}^μ are the momenta of the proton before and after the interaction. In order to improve legibility, we wrote out explicitly the auxiliary vectors p^μ , n^μ used in [12] in terms of their light-cone components. The variable ξ is known as skewedness (or skewness) and controls the longitudinal momentum transfer to the proton, α_{η_c} controls the fraction of the photon's light-cone momentum carried by η_c . In terms of these variables the invariant photon-proton energy is given by

$$S_{\gamma N} \equiv W^2 = (q + P_{\text{in}})^2 = s(1 + \xi) + m_N^2, \quad \sqrt{s} = \sqrt{\frac{W^2 - m_N^2}{1 + \xi}}. \quad (8)$$

The invariant momentum transfer to the proton

$$t = \Delta^2 = (P_{\text{out}} - P_{\text{in}})^2 = -\frac{1 + \xi}{1 - \xi} \Delta_{\perp}^2 - \frac{4\xi^2 m_N^2}{1 - \xi^2}. \quad (9)$$

We will also use the variables

$$u' = (p_{\eta_c} - q)^2, \quad t' = (k - q)^2, \quad M_{\gamma\eta_c}^2 = (k + p_{\eta_c})^2 \quad (10)$$

which are related as

$$-u' - t' = M_{\gamma\eta_c}^2 - M_{\eta_c}^2 - t. \quad (11)$$

Using definitions (10) and light-cone decomposition (1–6), it is possible to show that

$$\xi = \frac{M_{\gamma\eta_c}^2 - t}{2(W^2 - m_N^2) - M_{\gamma\eta_c}^2 + t} > 0, \quad s = W^2 - m_N^2 + \frac{t - M_{\gamma\eta_c}^2}{2} \quad (12)$$

The dependence on the variables $|\Delta_{\perp}|$, t is steeply decreasing in all the phenomenological models of GPDs, so the production of $\gamma\eta_c$ pairs predominantly occurs in the kinematics where $|\Delta_{\perp}|$, t are negligibly small. In this kinematics it is possible simplify the light-cone decomposition (1–6) and obtain the approximate relations

$$-t' \approx \alpha_{\eta_c} M_{\gamma\eta_c}^2 - M_{\eta_c}^2, \quad -u' \approx (1 - \alpha_{\eta_c}) M_{\gamma\eta_c}^2, \quad (13)$$

$$p_{\perp}^2 = \bar{\alpha}_{\eta_c} [\alpha_{\eta_c} M_{\gamma\eta_c}^2 - M_{\eta_c}^2] \approx -\bar{\alpha}_{\eta_c} t', \quad M_{\gamma\eta_c}^2 \approx 2s\xi \quad (14)$$

The algebraic constraint on the momenta of real photons

$$t' = (q - k)^2 = -2q \cdot k = -2|q||k|(1 - \cos \theta_{q,k}) \leq 0, \quad (15)$$

implies that the variable α_{η_c} is bound from below by $\alpha_{\eta_c} \geq M_{\eta_c}^2 / M_{\gamma\eta_c}^2$. For the variable u' , this constraint can be rewritten as

$$-u' \leq (-u')_{\max} = M_{\gamma\eta_c}^2 - M_{\eta_c}^2 - t. \quad (16)$$

We also may check that the pairwise invariant masses $(P_{\text{out}} + p_{\eta_c})^2$ and $(P_{\text{out}} + k)^2$ remain parametrically large, which implies that the produced η_c and γ are well-separated kinematically from the recoil proton. The evaluation of the amplitudes and cross-section will be performed below in the helicity basis, assuming that the polarization vector of any photon with momentum k and helicity λ is chosen in the light-cone gauge as

$$\varepsilon_T^{(\lambda=\pm 1)}(k) = \left(0, \frac{\varepsilon_{\lambda} \cdot k_{\perp}}{k^+}, \varepsilon_{\lambda} \right), \quad \varepsilon_{\lambda} = \frac{\hat{x} + i\lambda \hat{y}}{\sqrt{2}}. \quad (17)$$

The invariant photoproduction cross-section in terms of these variables may be represented as

$$\frac{d\sigma_{\gamma p \rightarrow \eta_c \gamma p}}{dt dt' dM_{\gamma\eta_c}} \approx \frac{\left| \mathcal{A}_{\gamma p \rightarrow \eta_c \gamma p}^{(\lambda,\sigma)} \right|^2}{128\pi^3 M_{\gamma\eta_c}} \quad (18)$$

where $\mathcal{A}_{\gamma p \rightarrow \eta_c \gamma p}^{(\lambda, \sigma)}$ is the amplitude of the process, and λ, σ are helicities of the incoming and outgoing photons. For the unpolarized beam of photons, a summation over helicities of photons in the final state and averaging over helicities in the initial state yields explicitly

$$\left| \mathcal{A}_{\gamma p \rightarrow \eta_c \gamma p}^{\text{(unpolarized)}} \right|^2 \equiv \frac{1}{2} \sum_{\lambda=\pm 1} \sum_{\sigma=\pm 1} \left| \mathcal{A}_{\gamma p \rightarrow \eta_c \gamma p}^{(\lambda, \sigma)} \right|^2 = \left| \mathcal{A}_{\gamma p \rightarrow \eta_c \gamma p}^{(+, +)} \right|^2 + \left| \mathcal{A}_{\gamma p \rightarrow \eta_c \gamma p}^{(+, -)} \right|^2. \quad (19)$$

The evaluation of the amplitude $\mathcal{A}_{\gamma p \rightarrow \eta_c \gamma p}^{(\lambda, \sigma)}$ may be performed in the collinear factorization picture, representing it as a convolution of the process-dependent perturbative partonic amplitude (the so-called coefficient function) and the target GPDs [2,3,5,29,30]. For scattering on the unpolarized nucleons, similar to (19), we should average over helicities of the incoming proton and sum over helicities of the final state, for this reason the result for the square of the amplitude may be represented as

$$\begin{aligned} \sum_{\text{spins}} \left| \mathcal{A}_{\gamma p \rightarrow \eta_c \gamma p}^{(\lambda, \sigma)} \right|^2 &= \left[4 \left(1 - \xi^2 \right) \left(\mathcal{H}_{\gamma \eta_c}^{(\lambda, \sigma)} \mathcal{H}_{\gamma \eta_c}^{(\lambda, \sigma)*} + \tilde{\mathcal{H}}_{\gamma \eta_c}^{(\lambda, \sigma)} \tilde{\mathcal{H}}_{\gamma \eta_c}^{(\lambda, \sigma)*} \right) \right. \\ &\quad - \xi^2 \left(\mathcal{H}_{\gamma \eta_c}^{(\lambda, \sigma)} \mathcal{E}_{\gamma \eta_c}^{(\lambda, \sigma)*} + \mathcal{E}_{\gamma \eta_c}^{(\lambda, \sigma)} \mathcal{H}_{\gamma \eta_c}^{(\lambda, \sigma)*} + \tilde{\mathcal{H}}_{\gamma \eta_c}^{(\lambda, \sigma)} \tilde{\mathcal{E}}_{\gamma \eta_c}^{(\lambda, \sigma)*} + \tilde{\mathcal{E}}_{\gamma \eta_c}^{(\lambda, \sigma)} \tilde{\mathcal{H}}_{\gamma \eta_c}^{(\lambda, \sigma)*} \right) \\ &\quad \left. - \left(\xi^2 + \frac{t}{4m_N^2} \right) \mathcal{E}_{\gamma \eta_c}^{(\lambda, \sigma)} \mathcal{E}_{\gamma \eta_c}^{(\lambda, \sigma)*} - \xi^2 \frac{t}{4m_N^2} \tilde{\mathcal{E}}_{\gamma \eta_c}^{(\lambda, \sigma)} \tilde{\mathcal{E}}_{\gamma \eta_c}^{(\lambda, \sigma)*} \right], \end{aligned} \quad (20)$$

and, inspired by similar analyses of other channels [31,32], we introduced shorthand notations

$$\mathcal{H}_{\gamma \eta_c}^{(\lambda, \sigma)}(\xi, t) = \int dx C_{\gamma \eta_c}^{(\lambda, \sigma)}(x, \xi) H_g(x, \xi, t), \quad (21)$$

$$\mathcal{E}_{\gamma \eta_c}^{(\lambda, \sigma)}(\xi, t) = \int dx C_{\gamma \eta_c}^{(\lambda, \sigma)}(x, \xi) E_g(x, \xi, t), \quad (22)$$

$$\tilde{\mathcal{H}}_{\gamma \eta_c}^{(\lambda, \sigma)}(\xi, t) = \int dx \tilde{C}_{\gamma \eta_c}^{(\lambda, \sigma)}(x, \xi) \tilde{H}_g(x, \xi, t), \quad (23)$$

$$\tilde{\mathcal{E}}_{\gamma \eta_c}^{(\lambda, \sigma)}(\xi, t) = \int dx \tilde{C}_{\gamma \eta_c}^{(\lambda, \sigma)}(x, \xi) \tilde{E}_g(x, \xi, t). \quad (24)$$

for the convolutions of the partonic amplitudes with different gluon GPDs $H_g, E_g, \tilde{H}_g, \tilde{E}_g$. For the gluon GPDs we use standard definitions from [2]

$$\begin{aligned} F^g(x, \xi, t) &= \frac{1}{\bar{P}^+} \int \frac{dz}{2\pi} e^{ix\bar{P}^+} \left\langle P' \left| G^{+\mu a} \left(-\frac{z}{2} n \right) \mathcal{L} \left(-\frac{z}{2}, \frac{z}{2} \right) G_\mu^{+a} \left(\frac{z}{2} n \right) \right| P \right\rangle = \\ &= \left(\bar{U}(P') \gamma_+ U(P) H^g(x, \xi, t) + \bar{U}(P') \frac{i\sigma^{+\alpha} \Delta_\alpha}{2m_N} U(P) E^g(x, \xi, t) \right), \end{aligned} \quad (25)$$

$$\begin{aligned} \tilde{F}^g(x, \xi, t) &= \frac{-i}{\bar{P}^+} \int \frac{dz}{2\pi} e^{ix\bar{P}^+} \left\langle P' \left| G^{+\mu a} \left(-\frac{z}{2} n \right) \mathcal{L} \left(-\frac{z}{2}, \frac{z}{2} \right) \tilde{G}_\mu^{+a} \left(\frac{z}{2} n \right) \right| P \right\rangle = \\ &= \left(\bar{U}(P') \gamma_+ \gamma_5 U(P) \tilde{H}^g(x, \xi, t) + \bar{U}(P') \frac{\Delta^+ \gamma_5}{2m_N} U(P) \tilde{E}^g(x, \xi, t) \right). \end{aligned} \quad (26)$$

$$\tilde{G}^{\mu\nu, a} \equiv \frac{1}{2} \epsilon^{\mu\nu\alpha\beta} G_{\alpha\beta}^a, \quad \mathcal{L} \left(-\frac{z}{2}, \frac{z}{2} \right) \equiv \mathcal{P} \exp \left(i \int_{-z/2}^{z/2} d\zeta A^+(\zeta) \right). \quad (27)$$

where U, \bar{U} are the spinors of the incoming and outgoing proton, and $G_{\mu\nu}$ is the operator of the gluonic field strength. In the light-cone gauge $A^+ = 0$ the Wilson link $\mathcal{L} = 1$, so the two-point gluon operators in (25) and (26) merely reduce to a product of two gluon fields, and thus \tilde{F}^g, F^g can be interpreted as helicity flip and helicity non-flip (unpolarized) probability amplitudes of the $gp \rightarrow gp$ subprocess.

In the reference frame (1)–(6) the dummy integration variable x in (21)–(24) is related to the light-cone components of the gluon $\ell_{\text{in}}^\mu, \ell_{\text{out}}^\mu$ before and after interaction

$$\ell_{\text{in}}^\mu = \left(0, (x + \xi)\sqrt{\frac{s}{2}}, \mathbf{0}_\perp\right), \quad \ell_{\text{out}}^\mu = \left(0, (x - \xi)\sqrt{\frac{s}{2}}, \Delta_\perp\right). \quad (28)$$

The partonic amplitudes $C_{\gamma\eta_c}^{(\lambda, \sigma)}$, $\tilde{C}_{\gamma\eta_c}^{(\lambda, \sigma)}$ can be evaluated perturbatively, taking into account the diagram shown in the Figure 1 with all possible permutations and disregarding small components of transverse momenta. In the leading order in α_s , the coefficient functions $C_{\gamma\eta_c}^{(\lambda, \sigma)}$ is given by a meromorphic function

$$C_{\gamma\eta_c}^{(\lambda,\sigma)}(x, \xi, \alpha_{\eta_c}, r) = \frac{\mathcal{N}^{(\lambda,\sigma)}(x, \xi, \alpha_{\eta_c}, r)}{(x + \xi - i0)(x - \xi + i0)(x + \kappa\xi - i0)(x - \kappa\xi + i0)}, \quad r = \frac{M_{\gamma\eta_c}}{M_{\eta_c}}, \quad (29)$$

where the numerator $\mathcal{N}^{(\lambda, \sigma)}(x, \xi, \alpha_{\eta_c}, r)$ is a lengthy polynomial function of its arguments which may be found in [12]. The poles of the function $C_{\eta_c}^{(\lambda, \sigma)}$ deserve special attention, since they determine the region which gives the dominant contribution in the convolution integrals (21)–(24). We may observe that in addition to classical poles $x = \pm \xi$, the coefficient function (29) includes a pair of new poles at $x = \pm \kappa \xi$, where

$$\kappa = 1 - \frac{1 - 1/r^2}{1 - \alpha_{\eta_c}/2} = \frac{1}{r^2} \frac{2 - \alpha_{\eta_c} r^2}{2 - \alpha_{\eta_c}}. \quad (30)$$

In the physically relevant kinematics ($r > 1$, $\alpha_{\eta_c} \in (M_{\eta_c}/M_{\gamma\eta_c}, 1)$) the values of κ are limited by $|\kappa| < 1$, so these new poles are located in the ERBL region. In the Figure 2 we have shown the density plot which illustrates the behavior of the coefficient function as a function of its arguments.

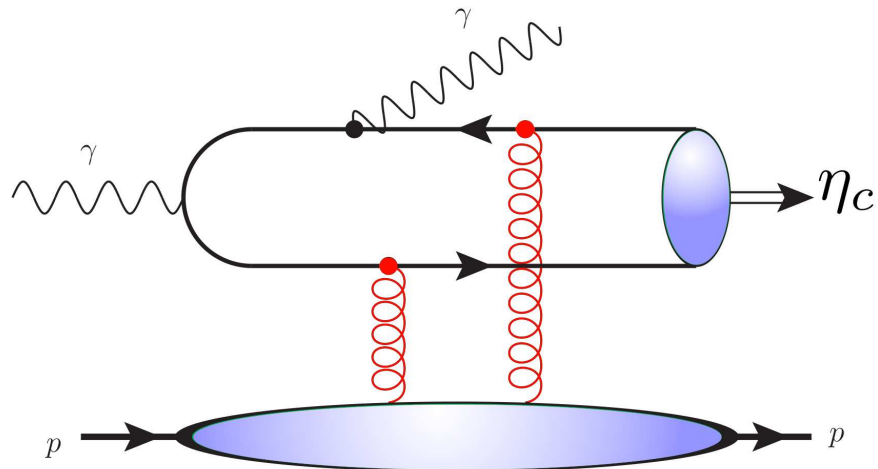


Figure 1. A typical diagram which contributes to $\eta_c \gamma$ photoproduction in the leading order in α_s . The full partonic-level amplitude $C_{\gamma\eta_c}^{(\lambda, \sigma)}$ includes a sum over all possible permutations of gluon and photon vertices ($4! = 24$ diagrams in total).

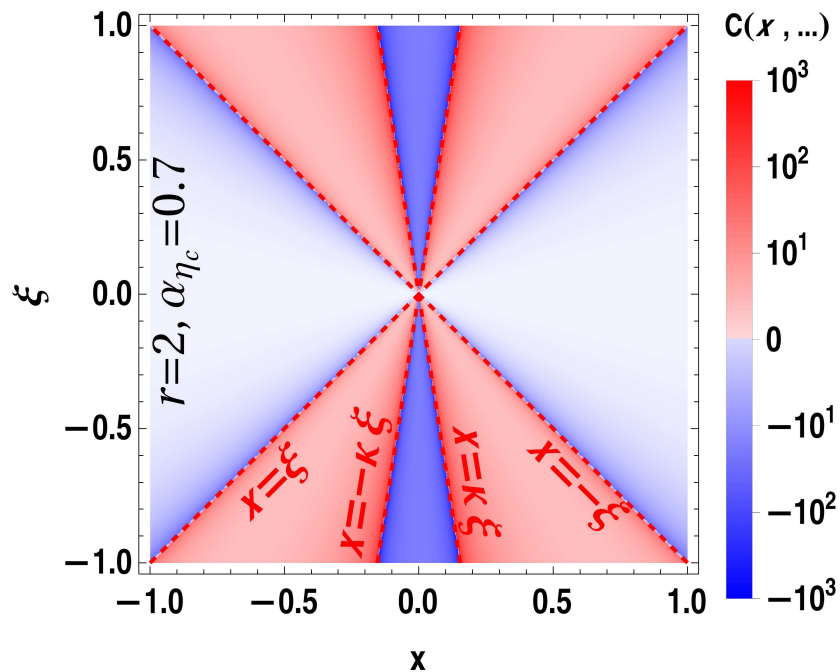


Figure 2. The density plot which illustrates the coefficient function $C_{\gamma\eta_c}^{(++)}$ (in relative units) as a function of variables x, ξ . Color intensity encodes the absolute value of the coefficient function, whereas a hue (red or blue) encodes the sign. The red dashed lines effectively demonstrate the position of the poles $x = \pm \xi, x = \pm \kappa \xi$ in the coefficient function (29). The value of the slope parameter κ depends on kinematics and is defined in (30).

3. Results

As could be seen from (21)–(24), the amplitude of the process is sensitive to various gluon GPDs. For the sake of definiteness, we will use the Kroll-Goloskokov parametrization [33–37] for our numerical estimates. The dominant contribution to the cross-section comes from the GPD $H_g(x, \xi, t)$. The differential cross-section of the process is shown in the Figures 3 and 4 as a function of kinematic variables $t, t', M_{\gamma\eta_c}$ and the photon-proton collision energy W . The dependence on each of these variables largely factorizes, namely, the shape of the kinematic dependence on each of the variables $t, t', M_{\gamma\eta_c}$ remains qualitatively the same for any choice of values of all the other variables. The sharply decreasing dependence on t in the collinear kinematics is entirely due to implemented parametrization of GPDs, and is common for all GPD parametrizations. Physically, this implies that the transverse momenta k_\perp^γ and $p_\perp^{\eta_c}$ are either oppositely directed to each other or negligibly small. In the right panel of the same Figure 3, we present the dependence of the cross-section on the variable t' . Similar to the previous case, the cross-section exhibits a rapid decrease as a function of this variable. As can be seen from (13), this dependence at a fixed $M_{\gamma\eta_c}$ is unambiguously linked to the α_{η_c} -dependence of the coefficient function (29).

In order to estimate the sensitivity of the suggested process to the choice of the GPD, in the lower row of the Figure 3 we compare side-by-side predictions obtained with the Kroll-Goloskokov parametrization [36,37] and the so-called zero-skewness parametrization, which assumes that gluon GPD is a product of the forward gluon PDF and nucleon form factor. For each parametrization we have shown predictions as a colored band, whose width reflects uncertainty due to higher order next-to-leading (NLO) corrections which were not taken into account, and was estimated varying the renormalization scale in the range $\mu \in (M_{\gamma\eta_c}/2, 2M_{\gamma\eta_c})$, as is usually done in the literature [2]. In the forward limit (small t) all the GPDs coincide with gluon PDF, so the sensitivity to the choice of the GPD

parametrization is minimal. At larger values of t , the two parametrizations of the GPDs differ significantly, leading to a completely different predictions for the cross-sections.

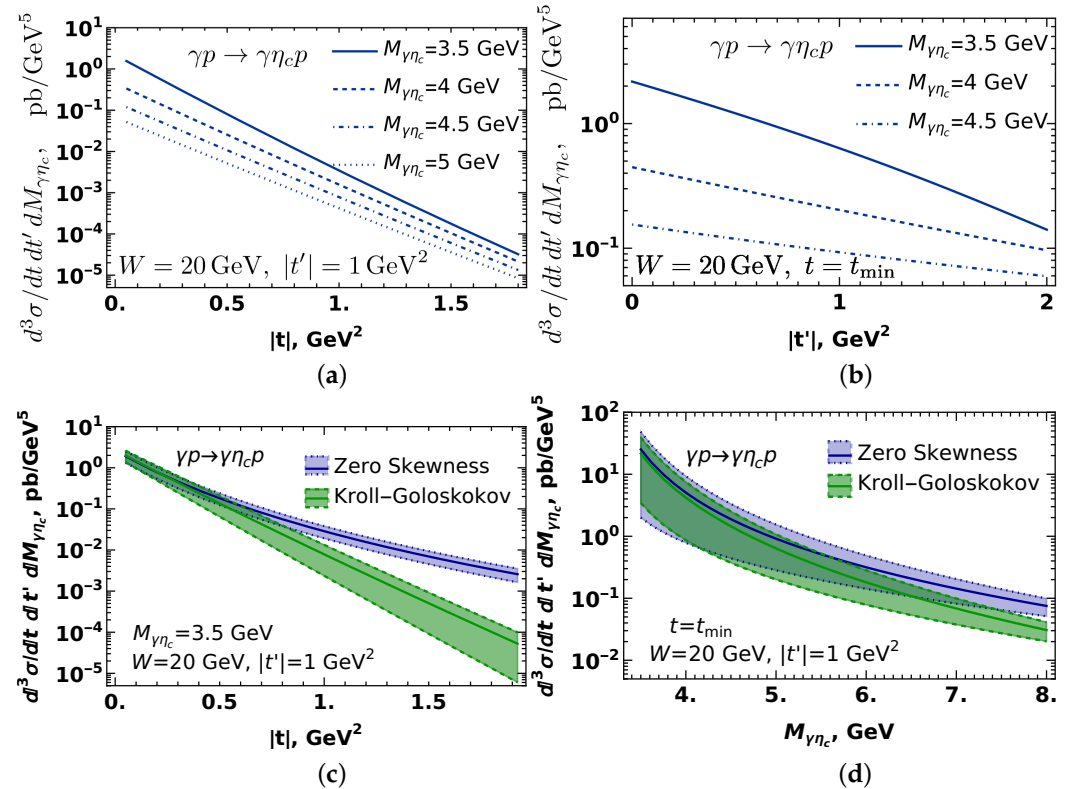


Figure 3. Dependence of the photoproduction cross-section (18) on different kinematic variables. (a) Dependence on the invariant momentum transfer t to the target (b) Dependence on the invariant variable t' defined in (10). (c,d) Comparison of predictions in Kroll-Goloskokov and Zero-Skewness parametrizations of the GPDs. The width of the band reflects the uncertainty due to NLO corrections and was obtained varying the renormalization scale in the range $\mu \in (M_{\gamma\eta_c}/2, 2M_{\gamma\eta_c})$.

In the left panel of the Figure 4 we have shown the dependence on invariant collision energy W . We observed that for all $t, t', M_{\gamma\eta_c}$ the differential cross-section grows with energy as

$$\frac{d\sigma^{\gamma p \rightarrow \gamma\eta_c p}}{dt dt' dM_{\gamma\eta_c}} \sim \left(\frac{W}{100 \text{ GeV}} \right)^\lambda, \quad 0.7 \leq \lambda \leq 0.8. \quad (31)$$

The energy W is closely related to dependence on the skewedness ξ defined in Equation (12). The latter variable determines position of the poles in the coefficient function $C_{\gamma\eta_c}^{(\lambda, \sigma)}(x, \xi, \alpha_{\eta_c}, r)$ defined in (29), and for this reason the observed W -dependence is a result of interplay of x - and ξ -dependence of the implemented GPDs. As could be seen from (12), in the kinematics $W \gg M_{\eta_c}$ the typical values of ξ are small, $\xi \sim M_{\gamma\eta_c}^2/2W^2 \ll 1$, and in the previous section we found that the dominant contribution to cross-section comes from the region $|x| \sim \xi \ll 1$. For this reason, we may relate the W -dependence of the cross-section with power law grows of the GPDs $H_g(x, \xi, t) \sim x^{-\delta_g}$ in the small- x domain [33]. Finally, the dependence on $M_{\gamma\eta_c}$ is due to explicit dependence of the coefficient function on this parameter, especially the position of the pole encoded in parameter κ in (30).

As we discussed earlier, the suggested approach is valid only at large invariant masses $M_{\gamma\eta_c}$, when the feed-down contributions are negligible. For this reason, for estimates of the total (fully integrated) cross-section we need to implement of the lower cutoff on the invariant mass $M_{\gamma\eta_c}$ when integrating over the phase space. For the sake of definiteness, we

will assume that this cutoff is given by $(M_{\gamma\eta_c})_{\min} \approx 3.5 \text{ GeV}$. Then the energy dependence of the fully integrated photoproduction cross-section is given by approximate relation

$$\sigma_{\text{tot}}^{\gamma p \rightarrow \gamma\eta_c p}(W, M_{\gamma\eta_c} \geq 3.5 \text{ GeV}) \approx 0.48 \text{ pb} \left(\frac{W}{100 \text{ GeV}} \right)^{0.75}, \quad (32)$$

in qualitative agreement with our earlier findings for the energy dependence of the differential cross-section (31).

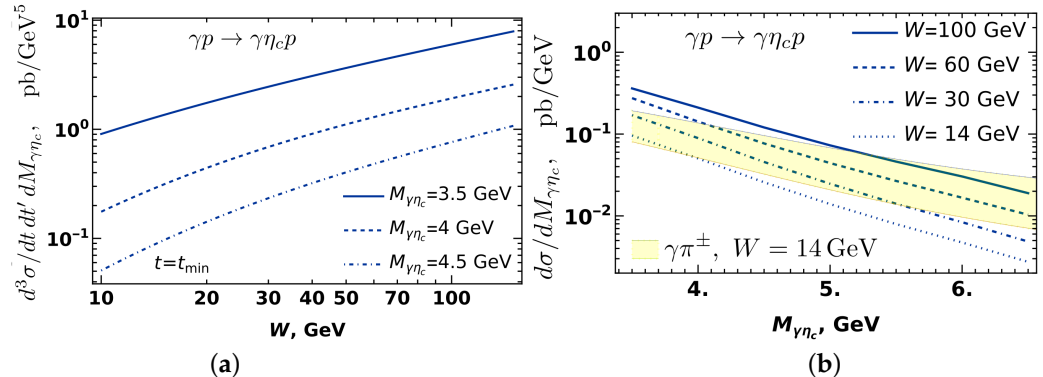


Figure 4. (a) Dependence of the cross-section (18) on the invariant photon-proton collision energy W . (b) Dependence of the single-differential cross-section on the invariant mass of $\eta_c\gamma$ pair at different collision energies. For comparison we added the cross-section of $\gamma p \rightarrow \gamma\pi^\pm n$ from [10] (light yellow band).

Finally, in the Table 1 we provide tentative estimates of the *electro* production of $\eta_c\gamma$ pairs in the EIC kinematics (the highest energy run). The smallness of the cross-section is largely due to a fine structure constant $\sim \alpha_{\text{em}}$ in the leptonic prefactor. For estimates of the production rate dN/dt and total number of events N we use the instantaneous luminosity $\mathcal{L} = 10^{34} \text{ cm}^{-2}\text{s}^{-1} = 10^{-5} \text{ fb}^{-1}\text{s}^{-1}$ and the integrated luminosity $\int dt \mathcal{L} = 100 \text{ fb}^{-1}$ [6,38,39], respectively. For estimates of the detection rate dN_d/dt and the total number of detected events N_d we assumed that the η_c quarkonia are detected via $\eta_c(1S) \rightarrow K_S^0 K^+ \pi^-$ decays with branching ratio [39,40]

$$\text{Br}_{\eta_c} = \text{Br}(\eta_c(1S) \rightarrow K_S^0 K^+ \pi^-) = 2.6\%. \quad (33)$$

Table 1. Estimates for the electroproduction of $\eta_c\gamma$ pairs in the EIC kinematics (highest energy run). Below $\sigma_{\text{tot}}^{ep \rightarrow e\gamma\eta_c p}$ is the electroproduction cross-section; dN/dt and N are the production rate and total number of produced $\eta_c\gamma$ pairs; similarly dN_d/dt and N_d are the detection rate and the total number of detected events (see the text for more details).

$\sqrt{s_{ep}}$	$\sigma_{\text{tot}}^{ep \rightarrow e\gamma\eta_c p}$	Production Rates		Counting Rates	
		N	dN/dt	N_d	dN_d/dt
141 GeV	49 fb	4.9×10^3	42/day	127	32/month

4. Discussion and Conclusions

In this paper we analyzed the production of $\eta_c\gamma$ production in the collinear factorization approach and demonstrated that it is possible to use this channel for studies of the gluon GPDs. The coefficient function of this process is a simple meromorphic function with a two pairs of poles in the ERBL region. While the analytic structure of the coefficient function does not allow direct extraction of the GPDs from the amplitude, the suggested process can be used to constrain the parametrizations of the gluon GPDs (especially unpolarized GPD H_g). The photoproduction cross-section of $\eta_c\gamma$ numerically is on par with that

of $\gamma\pi$, $\gamma\rho$ pairs if compared at the same invariant meson-photon masses. However, the total (integrated) cross-section is below a picobarn due to inherently large mass of the $\gamma\eta_c$ pair. Despite of this, we expect a production rate of several thousand $\eta_c\gamma$ pairs per 100 fb^{-1} of integrated luminosity. The cross-section increases with energy and could be significant for TeV-range photon-proton collisions, though the approach becomes less reliable in that kinematics due to large NLO corrections and saturation effects. We expect that the suggested process could be studied in ultraperipheral collisions at LHC, in electron-proton collisions at the future Electron Ion Collider (EIC) [5,6,38] and possibly at JLAB after future 22 GeV upgrade [41]. While the expected number of produced $\eta_c\gamma$ apparently is sufficient for experimental study in all these setups, a systematic study of various backgrounds may be needed to make conclusions about experimental feasibility of this channel for future analysis. The most concerning are the *inclusive* η_c production channels, since they do not require C-odd exchanges in t -channel, and thus could constitute a sizeable background which potentially could set the detection thresholds.

Funding: This research was funded by ANID PIA/APOYO AFB230003 (Chile) and ANID Fondecyt (Chile) grants 1220242, 1251975. “Powered@NLHPC: This research was partially supported by the supercomputing infrastructure of the NLHPC (ECM-02)”.

Institutional Review Board Statement: Not applicable, since the study does not involve humans or animals.

Data Availability Statement: Data is contained within the article. Additional predictions (e.g., estimates of the cross-section in other kinematics) may be obtained on request from the author.

Conflicts of Interest: The author declares no conflicts of interest which may be perceived as inappropriately influencing the representation or interpretation of reported research results. The funders had no role in the design of the study; in the collection, analyses, or interpretation of data; in the writing of the manuscript; or in the decision to publish the results.

References

1. Goeke, K.; Polyakov, M.V.; Vanderhaeghen, M. Hard exclusive reactions and the structure of hadrons. *Prog. Part. Nucl. Phys.* **2001**, *47*, 401. [\[CrossRef\]](#)
2. Diehl, M. Generalized parton distributions. *Phys. Rept.* **2003**, *388*, 41. [\[CrossRef\]](#)
3. Guidal, M.; Moutarde, H.; Vanderhaeghen, M. Generalized Parton Distributions in the valence region from Deeply Virtual Compton Scattering. *Rept. Prog. Phys.* **2013**, *76*, 066202. [\[CrossRef\]](#) [\[PubMed\]](#)
4. Dutrieux, H.; Lorcé, C.; Moutarde, H.; Sznajder, P.; Trawinski, A.; Wagner, J. Phenomenological assessment of proton mechanical properties from deeply virtual Compton scattering. *Eur. Phys. J. C* **2021**, *81*, 300. [\[CrossRef\]](#)
5. Burkert, V.; Elouadrhiri, L.; Afanasev, A.; Arrington, J.; Contalbrigo, M.; Cosyn, W.; Deshpande, A.; Glazier, D.; Ji, X.; Liuti, S.; et al. Precision Studies of QCD in the Low Energy Domain of the EIC. *arXiv* **2002**, arXiv:2211.15746. [\[CrossRef\]](#)
6. Khalek, R.A.; Accardi, A.; Adam, J.; Adamiak, D.; Akers, W.; Albaladejo, M.; Al-Bataineh, A.; Alexeev, M.G.; Ameli, F.; Antonioli, P.; et al. Science Requirements and Detector Concepts for the Electron-Ion Collider: EIC Yellow Report. *arXiv* **2021**, arXiv:2103.05419.
7. Kumericki, K.; Liuti, S.; Moutarde, H. GPD phenomenology and DVCS fitting: Entering the high-precision era. *Eur. Phys. J. A* **2016**, *52*, 157. [\[CrossRef\]](#)
8. Bertone, V.; Dutrieux, H.; Mezrag, C.; Moutarde, H.; Sznajder, P. Deconvolution problem of deeply virtual Compton scattering. *Phys. Rev. D* **2021**, *103*, 114019. [\[CrossRef\]](#)
9. Moffat, E.; Freese, A.; Cloët, I.; Donohoe, T.; Gamberg, L.; Melnitchouk, W.; Metz, A.; Prokudin, A.; Sato, N. Shedding light on shadow generalized parton distributions. *Phys. Rev. D* **2023**, *108*, 036027. [\[CrossRef\]](#)
10. Duplančić, G.; Nabeebaccus, S.; Paszek-Kumerički, K.; Pire, B.; Szymanowski, L.; Wallon, S. Accessing chiral-even quark generalised parton distributions in the exclusive photoproduction of a $\gamma\pi^\pm$ pair with large invariant mass in both fixed-target and collider experiments. *J. High Energy Phys.* **2023**, *03*, 241. [\[CrossRef\]](#)
11. Duplančić, G.; Paszek-Kumerički, K.; Pire, B.; Szymanowski, L.; Wallon, S. Probing axial quark generalized parton distributions through exclusive photoproduction of a $\gamma\pi^\pm$ pair with a large invariant mass. *J. High Energy Phys.* **2018**, *11*, 179. [\[CrossRef\]](#)
12. Siddikov, M. Exclusive photoproduction of $\eta_c\gamma$ pairs with large invariant mass. *Phys. Rev. D* **2024**, *110*, 056043. [\[CrossRef\]](#)

13. Boussarie, R.; Pire, B.; Szymanowski, L.; Wallon, S. Exclusive photoproduction of a $\gamma\rho$ pair with a large invariant mass. *J. High Energy Phys.* **2017**, *2*, 54; Erratum in *J. High Energy Phys.* **2018**, *10*, 29.

14. Cosyn, W.; Pire, B. Diffractive rho plus lepton pair production at an electron-ion collider. *Phys. Rev. D* **2021**, *103*, 114002. [\[CrossRef\]](#)

15. Pedrak, A.; Pire, B.; Szymanowski, L.; Wagner, J. Electroproduction of a large invariant mass photon pair. *Phys. Rev. D* **2020**, *101*, 114027. [\[CrossRef\]](#)

16. Pire, B.; Szymanowski, L.; Wallon, S. Diffractive deeply virtual Compton scattering. *Phys. Rev. D* **2020**, *101*, 074005. [\[CrossRef\]](#)

17. Pedrak, A.; Pire, B.; Szymanowski, L.; Wagner, J. Hard photoproduction of a diphoton with a large invariant mass. *Phys. Rev. D* **2017**, *96*, 074008. [\[CrossRef\]](#)

18. Beiyad, M.E.; Pire, B.; Segond, M.; Szymanowski, L.; Wallon, S. Photoproduction of a $\pi\rho T$ pair with a large invariant mass and transversity generalized parton distribution. *Phys. Lett. B* **2010**, *688*, 154. [\[CrossRef\]](#)

19. Ivanov, D.Y.; Pire, B.; Szymanowski, L.; Teryaev, O.V. Probing chiral-odd GPDs in diffractive electroproduction of two vector mesons. *Phys. Lett. B* **2002**, *550*, 65. [\[CrossRef\]](#)

20. Duplančić, G.; Nabeebaccus, S.; Paszek-Kumerički, K.; Pire, B.; Szymanowski, L.; Wallon, S. Accessing GPDs through the exclusive photoproduction of a photon-meson pair with a large invariant mass. *arXiv* **2022**, arXiv:2212.01034.

21. Qiu, J.W.; Yu, Z. Extracting transition generalized parton distributions from hard exclusive pion-nucleon scattering. *Phys. Rev. D* **2024**, *109*, 074023. [\[CrossRef\]](#)

22. Qiu, J.W.; Yu, Z. Extraction of the Parton Momentum-Fraction Dependence of Generalized Parton Distributions from Exclusive Photoproduction. *Phys. Rev. Lett.* **2023**, *131*, 161902. [\[CrossRef\]](#) [\[PubMed\]](#)

23. Deja, K.; Martinez-Fernandez, V.; Pire, B.; Sznajder, P.; Wagner, J. Phenomenology of double deeply virtual Compton scattering in the era of new experiments. *Phys. Rev. D* **2023**, *107*, 094035. [\[CrossRef\]](#)

24. Siddikov, M.; Schmidt, I. Exclusive production of quarkonia pairs in collinear factorization framework. *Phys. Rev. D* **2023**, *107*, 034037. [\[CrossRef\]](#)

25. Siddikov, M.; Schmidt, I. Exclusive photoproduction of D-meson pairs with large invariant mass. *Phys. Rev. D* **2023**, *108*, 096031. [\[CrossRef\]](#)

26. Bodwin, G.T.; Braaten, E.; Lepage, G.P. Rigorous QCD analysis of inclusive annihilation and production of heavy quarkonium. *Phys. Rev. D* **1995**, *51*, 1125. Erratum in *Phys. Rev. D* **1997**, *55*, 5853. [\[CrossRef\]](#)

27. Maltoni, F.; Mangano, M.L.; Petrelli, A. Quarkonium photoproduction at next-to-leading order. *Nucl. Phys. B* **1998**, *519*, 361. [\[CrossRef\]](#)

28. Brambilla, N.; Eidelman, S.; Heltsley, B.K.; Vogt, R.; Bodwin, G.T.; Eichten, E.; Frawley, A.D.; Meyer, A.B.; Mitchell, R.E.; Papadimitriou, V.; et al. Heavy quarkonium: Progress, puzzles, and opportunities. *Eur. Phys. J. C* **2011**, *71*, 1534.

29. Diehl, M.; Feldmann, T.; Jakob, R.; Kroll, P. The overlap representation of skewed quark and gluon distributions. *Nucl. Phys. B* **2001**, *596*, 33. Erratum in *Nucl. Phys. B* **2001**, *605*, 647. [\[CrossRef\]](#)

30. Boer, D.; Diehl, M.; Milner, R.; Venugopalan, R.; Vogelsang, W.; Accardi, A.; Aschenauer, E.; Burkardt, M.; Ent, R.; Guzey, V.; et al. Gluons and the quark sea at high energies: Distributions, polarization, tomography. *arXiv* **2011**, arXiv:1108.1713.

31. Belitsky, A.V.; Mueller, D.; Kirchner, A. Theory of deeply virtual Compton scattering on the nucleon. *Nucl. Phys. B* **2002**, *629*, 323. [\[CrossRef\]](#)

32. Belitsky, A.V.; Radyushkin, A.V. Unraveling hadron structure with generalized parton distributions. *Phys. Rept.* **2005**, *418*, 1–387. [\[CrossRef\]](#)

33. Goloskokov, S.V.; Kroll, P. The Longitudinal cross-section of vector meson electroproduction. *Eur. Phys. J. C* **2007**, *50*, 829. [\[CrossRef\]](#)

34. Goloskokov, S.V.; Kroll, P. The Role of the quark and gluon GPDs in hard vector-meson electroproduction. *Eur. Phys. J. C* **2008**, *53*, 367. [\[CrossRef\]](#)

35. Goloskokov, S.V.; Kroll, P. The target asymmetry in hard vector-meson electroproduction and parton angular momenta. *Eur. Phys. J. C* **2009**, *59*, 809. [\[CrossRef\]](#)

36. Goloskokov, S.V.; Kroll, P. An attempt to understand exclusive π^+ electroproduction. *Eur. Phys. J. C* **2010**, *65*, 137. [\[CrossRef\]](#)

37. Goloskokov, S.V.; Kroll, P. Transversity in hard exclusive electroproduction of pseudoscalar mesons. *Eur. Phys. J. A* **2011**, *47*, 112. [\[CrossRef\]](#)

38. Accardi, A.; Albacete, J.L.; Anselmino, M.; Armesto, N.; Aschenauer, E.C.; Bacchetta, A.; Boer, D.; Brooks, W.K.; Burton, T.; Chang, N.B.; et al. Electron-Ion Collider: The next QCD frontier: Understanding the glue that binds us all. *Eur. Phys. J. A* **2016**, *52*, 268. [\[CrossRef\]](#)

39. Navas, S.; Amsler, C.; Gutsche, T.; Hanhart, C.; Hernández-Rey, J.J.; Lourenço, C.; Masoni, A.; Mikhasenko, M.; Mitchell, R.E.; Patrignani, C.; et al. Review of particle physics. *Phys. Rev. D* **2024**, *110*, 030001. [\[CrossRef\]](#)

40. Ablikim, M.; Achasov, M.N.; Ahmed, S.; Albrecht, M.; Alekseev, M.; Amoroso, A.; An F.F.; An Q.; Bai, Y.; Bakina, O.; et al. Measurements of the branching fractions of $\eta_c \rightarrow K^+ K^- \pi^0$, $K_S^0 K^\pm \pi^\mp$, $2(\pi^+ \pi^- \pi^0)$, and $p\bar{p}$. *Phys. Rev. D* **2019**, *100*, 012003. [[CrossRef](#)]

41. Accardi, A.; Achenbach, P.; Adhikari, D.; Afanasev, A.; Akondi, C.S.; Akopov, N.; Albaladejo, M.; Albataineh, H.; Albrecht, M.; Almeida-Zamora, B.; et al. Strong Interaction Physics at the Luminosity Frontier with 22 GeV Electrons at Jefferson Lab. *Eur. Phys. J. A* **2024**, *60*, 173. [[CrossRef](#)]

Disclaimer/Publisher’s Note: The statements, opinions and data contained in all publications are solely those of the individual author(s) and contributor(s) and not of MDPI and/or the editor(s). MDPI and/or the editor(s) disclaim responsibility for any injury to people or property resulting from any ideas, methods, instructions or products referred to in the content.